Systematic and Material Independent Variation of Electrical, Optical, and Chemical Properties of Ln Materials over the Ln Series (Ln = La, Ce, Pr, ..., Lu)

E. van der Kolk* and P. Dorenbos

Faculty of Applied Sciences, Delft University of Technology, Mekelweg 15, 2629 JB Delft, The Netherlands

Received April 3, 2006. Revised Manuscript Received May 23, 2006

A universal model for lanthanide (Ln) materials is presented that describes a systematic and material independent variation of the electronic structure over the Ln series (La, Ce, Pr, ..., Lu). The model is derived from experimental data on 4f and 5d energies of Ln ions as impurities in luminescent materials but, as will be shown, can fruitfully be applied to stoichiometric Ln materials as well. The validity and usefulness of the model is demonstrated by application to the Ln sulfides and the well-known Ln oxides LnO, Ln_2O_3, and LnO_2 for which the model correctly predicts insulating, semiconducting, or metallic behavior, nature, and magnitude of band gap energies and chemical stability of Ln materials as well as valence and valence changes of Ln ions. The model may serve as a reliable tool to accelerate design of a broad range of Ln materials with deliberately chosen properties.

1. Introduction

Lanthanide (Ln)-doped or stoichiometric Ln materials play an increasingly important role in photonic applications such as lasers,[1] wide band gap electroluminescent devices,[2,3] light-emitting diode phosphors,[4] and scintillator detectors.[5] They are also considered for future applications based on spintronics[6] or high-density optical or magnetic data storage.[7] Besides these applications, Ln materials are at the focal point of solid-state research into a variety of fundamental phenomena such as metal−insulator transitions, colossal magnetoresistance, and valence transitions or charge ordering.[8−12]

The wide variety of electrical, optical, and chemical properties and applications of Ln materials is to a large extent controlled by the relative energy and inherently different nature of the 4f and 5d electrons of the Ln ions. Ln ions in compounds have either a $4f^n$ or a $4f^{n-1}5d^1$ ground-state electron configuration. The $4f^n$ configuration has *n* strongly correlated and localized corelike 4f electrons whose energies are to a good approximation unaffected by the Ln ion crystalline environment but strongly change as a function of the type of Ln ion over the Ln series. The 5d electrons have an entirely different character. Their energy strongly depends on the type of Ln environment but not on the type of Ln ion. In addition, the 5d orbitals are highly delocalized and form the conduction band (CB) in concentrated systems.

Considerable progress has been made in the past few years in developing models describing the energy of the 4f and 5d states, both ab initio based as well as empirical based. These models predict Ln material properties by considering the energy of the 4f and 5d states as a function of the type of Ln ion of the Ln series (La, Ce, Pr, ..., Lu). Strange et al.[13] were able to compute Ln valencies and valence changes for the Ln metals and their sulfides on an ab initio basis by total energy calculations for all the Ln ions in the divalent and trivalent states. Petit et al.[14] applied the same method to compute the valencies and band gaps of the oxides of Ce, Pr, Nd, Pm, Sm, Eu, Gd, Tb, Dy, and Ho.

Alternatively, Dorenbos developed empirical based models for Ln-ion-doped (luminescent) materials.[15−18] These models describe and predict the energy between the 5d excited state and the 4f ground state as a function of the type of Ln ion.[15,16] Later these models were extended to involve the energy of the 4f and 5d states relative to the valence band (VB) and CB.[17,18] Because the wide variety of luminescence properties of Ln-doped materials is to a large extent controlled by the

* To whom correspondence should be addressed. E-mail: e.vanderkolk@tnw.tudelft.nl. Tel.: +31 152783464. Fax: +31 152786422.

(1) Lage, M. M.; Moreira, R. L.; Matinaga, F. M.; Gesland, J.-Y. *Chem. Mater.* **2005**, *17*, 4523.
(2) Quang, Y. Q.; Steckle, A. J. *Appl. Phys. Lett.* **2003**, *82*, 502.
(3) Steckle, A. J.; Zavada, J. M. *MRS Bull.* **1999**, *24*, 16.
(4) Mueller-Mach, R.; Mueller, G.; Krames, M. R.; Hoppe, H. A.; Stadler, F.; Schnick, W.; Juestel, T.; Schmidt P. *Phys. Status Solidi* **2005**, *202*, 1727.
(5) van Loef, E. V. D.; Dorenbos, P.; van Eijk, C. W. E.; Kramer, K.; Gudel, H. U. *Appl. Phys. Lett.* **2001**, *79*, 1573.
(6) LeClair, P.; Ha, J. K.; Swagten, H. J. M.; Kohlhepp, J. T.; van de Vin, C. H.; de Jonge, W. J. M. *Appl. Phys. Lett.* **2002**, *80*, 625.
(7) Tsunashima, S. *J. Phys. D* **2001**, *34*, R87.
(8) Hoekstra, A. F. T.; Roy, A. S.; Rosenbaum, T. F.; Griessen, R.; Wijngaarden, R. J.; Koeman, N. J. *Phys. Rev. Lett.* **2001**, *86*, 5349.
(9) Prellier, W.; Lecoeur, P.; Mercey, B. *J. Phys.: Condens. Matter* **2001**, *13*, R915.
(10) Arvanitidis, J.; Papagelis, K.; Margadonna, S.; Prassides, K.; Fitch, A. N. *Nature* **2003**, *425*, 599.
(11) Rao, C. N. R.; Arulraj, A.; Cheetham, A. K.; Raveau, B. *J. Phys.: Condens. Matter* **2000**, *12*, R83.
(12) Steeneken, P. G.; Tjeng, L. H.; Elfimov, I.; Sawatzky, G. A.; Ghiringhelli, G.; Brookes, N. B.; Huang, D. J. *Phys. Rev. Lett.* **2002**, *88*, 047201.
(13) Strange, P.; Svane, A.; Temmerman, W. M.; Szotek, Z.; Winter, H. *Nature* **1999**, *399*, 756.
(14) Petit, L.; Svane, A.; Szotek, Z.; Temmerman, W. M. *Phys. Rev. B* **2005**, *72*, 205118.
(15) Dorenbos, P. *J. Lumin.* **2000**, *91*, 91 and 155.
(16) Dorenbos, P. *J. Phys.: Condens. Matter* **2003**, *15*, 575.
(17) Dorenbos, P. *J. Phys.: Condens. Matter* **2003**, *15*, 8417.
(18) Dorenbos, P. *J. Lumin.* **2004**, *108*, 301.

10.1021/cm060775s CCC: $33.50
Published on Web 06/23/2006

energy difference between the 4f and the 5d states and on their location relative to the VB and CB, these models are highly practical in describing and predicting temperature quenching, charge trapping, and energy transfer processes in luminescent materials. These empirical models are now actively used also by other material scientists.[19−22]

We realize that the models developed for Ln-doped materials may also be applied to stoichiometric (fully concentrated) Ln materials like EuO, CeO_2, or SmS and many more nonbinary Ln materials. In this work it is demonstrated that the variation over the Ln series of the 4f and the 5d energies relative to the VB in Ln-doped materials shows a systematic and material independent behavior. This universal behavior is then used to construct a model for fully concentrated Ln materials that predicts the electronic structure of all the members of a specific Ln material when that of only one is known. The validity of the model will be demonstrated by application to the well-known Ln monosulfides (LnS) and the Ln oxides LnO, Ln_2O_3, and LnO_2.

2. Experimental Data

The construction of a model for fully concentrated Ln materials has become possible as a result of a recently completed review of the electronic structure of more than 500 Ln-ion-doped inorganic materials.[15,16] An important conclusion of that review is that the variation over the Ln series in energy difference $E_{4f\rightarrow 5d}$, between the Ln ion 4f ground state and the lowest energy 5d state, follows a characteristic double-seated shape that is independent of the type of host material and Ln valence state. The variation in $E_{4f\rightarrow 5d}$ is plotted in the top panel of Figure 1 for the divalent and the trivalent Ln ions. Note that the two curves were shifted to zero energy at $n = 1$ because the variation in energy is of interest here and not the absolute value. It can be observed that both curves show a characteristic "double-seated" shape that deviate no more then about 0.2 eV from each other.

A second conclusion of the work by Dorenbos is that the variation over the Ln series of the energy difference between the Ln 4f ground state and the top of the VB shows a very similar but mirrored double-seated shape[17,18] as can be seen by the + symbols in the lower panel Figure 1. The latter conclusion was derived from a systematic study of ligand to metal charge transfer (CT) energies in a large number of Ln-doped materials.[17,18] These CT energies of Ln^{3+} ions provide the location of the 4f ground state of Ln^{2+} ions above the VB.[17,23]

The double-seated shape of the 4f energies is also observed in sparsely available systematic electron spectroscopy studies [X-ray photoelectron spectroscopy (XPS), UV photoelectron spectroscopy (UPS), and X-ray Bremsstrahlung isochromat spectroscopy (XBIS)] that have provided the 4f binding energy of (almost) all Ln ions in the same material. Lang et al.[24] established the energy of 4f levels of divalent and trivalent Ln ions in the Ln metals combining XPS and XBIS techniques. Thiel et al.[25] studied 4f energies by using UPS in the Ln-ion-doped garnets $Y_3Al_5O_{12}$ for trivalent Ln ions ranging from Gd^{3+} to Lu^{3+}. Thompson et al.[26] studied the systematical behavior of 4f level energies of trivalent Gd, Dy, Er, and Yb in organic complexes by XPS. The lower panel Figure 1 includes 4f binding energies of divalent (black crosses) and trivalent (red crosses) Ln ions in the Ln metals and the garnet insulators $Y_3Al_5O_{12}$ (orange crosses) and Ln^{3+} impurities in inorganic insulators and semiconductors (green plus signs) and in the Ln−tris-8-hydroxyquinolines (black plus signs). Again all curves were shifted to zero energy at $n = 1$ to be able to compare the variation in 4f energies of the different materials over the Ln series. Despite the intrinsically different natures of these materials (inorganic, organic, and metallic) the double-seated shape is the same each time.

The shape of the 4f binding energies can be derived from the 4f binding energies of the free Ln ions that is well-understood (see ref 16 and references therein). It was shown by Pedrini et al.[27] and later by Thiel et al.[28] that the variation

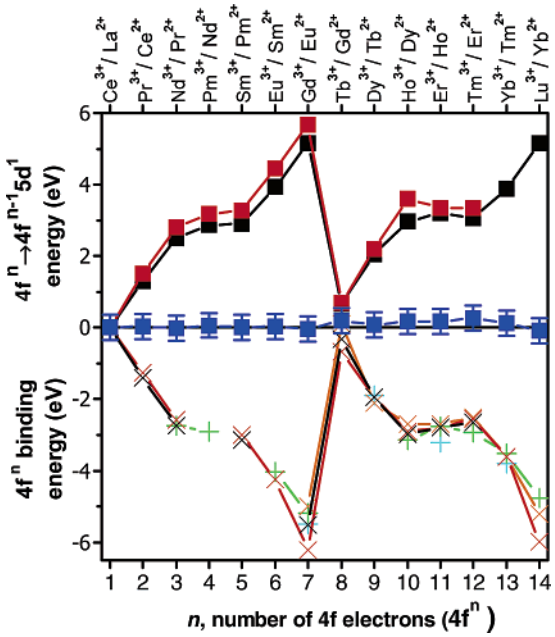

Figure 1. Upper panel: Variation in energy over the Ln series (La, Ce, Pr, ..., Lu) of the lowest energy $4f^n \rightarrow 4f^{n-1}5d^1$ transition of Ln^{2+} (black boxes) and Ln^{3+} (red boxes) impurities in inorganic insulators and semiconductors. Lower panel: Variation in energy of the lowest energy $4f^n$ binding energy of Ln^{2+} (black crosses) and Ln^{3+} (red crosses) ions in the Ln metals, Ln^{3+} ions in $Y_3Al_5O_{12}$ (orange crosses), Ln^{3+} ions in Ln organic complexes (black plus signs), and Ln^{3+} impurities in inorganic insulators and semiconductors (green plus signs). ■ symbols represent the calculated binding energy of the lowest energy $4f^{n-1}5d^1$ state. All curves were shifted to zero energy at $n = 1$.

(19) Liu, G. K.; Jensen, M. P.; Almond, P. M. *J. Chem. Phys* **2006**, *110*, 2081.
(20) Aitasalo, T.; Holsa, J.; Jungner, H.; Lastusaari, M.; Niittykoski, J. *J. Phys. Chem. B* **2006**, *110*, 4589.
(21) Yamaga, M.; Masui, Y.; Sakuta, S. *Phys. Rev. B* **2005**, *71*, 205102.
(22) Yen, W. M. *Phys. Solid State* **2005**, *47*, 1393.
(23) Wong, W. C.; McClure, D. S.; Basun, S. A.; Kokta, M. R. *Phys. Rev. B* **1995**, *51*, 5682.
(24) Lang, J. K.; Baer, Y.; Cox, P. A. *Phys. Rev. Lett.* **1979**, *42*, 74.
(25) Thiel, C. W.; Cruguel, H.; Wu, H.; Sun, Y.; Lapeyre, G. J.; Cone, R. L.; Equall, R. W.; Macfarlane, R. M. *Phys. Rev. B* **2001**, *64*, 085107.
(26) Thompson, J.; Arima, V.; Zou, Y.; Fink, R.; Umbach, E.; Cingolani, R.; Blyth, R. I. R. *Phys. Rev. B* **2004**, *70*, 153104.
(27) Pedrini, C.; McClure, D. S.; Anderson, C. A. *J. Chem. Phys.* **1979**, *70*, 4959.
(28) Thiel, C. W.; Cruguel, H.; Sun, Y.; Lapeyre, G. J.; Macfarlane, R. M.; Equall, R. W.; Cone, R. L. *J. Lumin.* **2001**, *94*, 1.

in 4f binding energy E(Ln), over the Ln series in Ln-doped systems, differs from that of the free Ln ions $E(\mathrm{Ln})_{\mathrm{free}}$ by a Ln ion radius (R) dependent term equal to $\alpha_R(R_0 - R)$, that is,

$$E(\mathrm{Ln}) = E(\mathrm{Ln})_{\mathrm{free}} - \alpha_R(R_0 - R)$$

in which R_0 is the ionic radius of the ion replaced by the Ln ion and α_R is a proportionality constant[28] representing the strength of the in-material 4f binding energy change. The data presented in the lower panel of Figure 1 shows that α_R is, within the experimental error, material and Ln valence state independent. This means that once the 4f binding energy is known for one Ln ion in a any specific material, the 4f binding energy of all other Ln ions can be predicted for that material.

Although some systematic experimental studies on the absolute location of 4f levels of Ln ions in materials exist (see lower panel of Figure 1), no studies providing the 5d binding energies were found. There is, however, a powerful method to calculate the 5d binding energies that was recently applied for the first time by Thiel et al.[28] in the case of the Ln-ion-doped wide band gap material $Y_3Al_5O_{12}$.[28] By adding the Ln ion 4f → 5d transition energies to the 4f binding energies, that is, adding the averaged values in the upper and lower panels in Figure 1, the 5d binding energies are obtained. The 5d energies calculated in this way are displayed by the ■ symbols in Figure 1. It appears that the 5d binding energies are constant across the Ln series well within 0.5 eV, which is considered as the typical experimental error in the electron or optical spectroscopy data used.

It can be concluded from Figure 1 that the 4f and 5d energies relative to the VB show a universal and systematic behavior that is independent of the type of material and the Ln valence state. It also suggests that the systematic behavior is independent of the Ln concentration and might be applicable to fully concentrated, stoichiometric Ln materials. In the rest of this article we show that this is indeed the case by application to the well-known Ln monosulfides (LnS) and the Ln oxides LnO, Ln_2O_3, and LnO_2 for which basic electrical, optical, and chemical properties are correctly predicted.

3. Results and Discussion

3.1. Lanthanide Monosulfide LnS. In Figure 2 the model is tested by application to the well-studied Ln monosulfide, LnS. The left panel of this figure schematically represents the density of states in EuS. The ligand S^{2-} 3p-derived VB, the localized Eu^{2+} $4f^7$ ground state, and the Eu^{2+} 5d-derived CB band (split into a 5d t_{2g} and 5d e_g state in the cubic crystal field of EuS) are plotted. Their relative energies were taken from the data of Wachter.[29] The horizontal dashed lines connect these data to the right panel of Figure 2 where the top of the VB, 4f ground state, and bottom of the 5d CB energies are represented by a square, a triangle, and a circle, respectively, at $n + m = 7$. Here we have adopted the common notation $4f^n5d^m$ for the electron configuration of

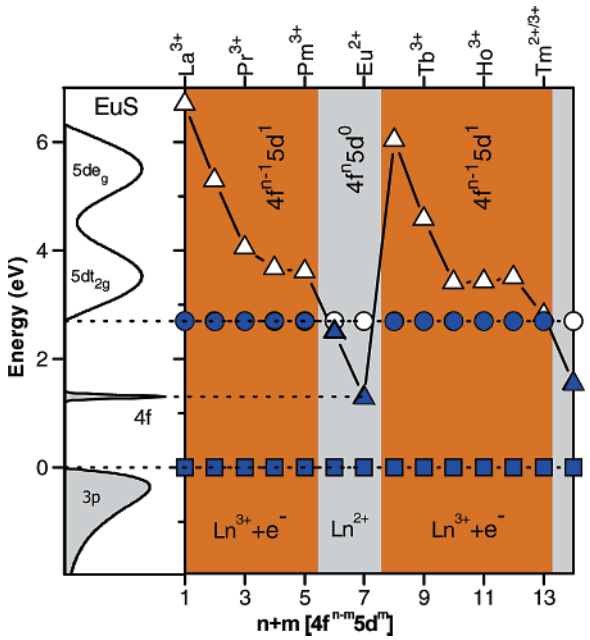

Figure 2. Left panel: Schematic representation of the density of states of the sulfur 3p-derived VB, the localized Eu $4f^7$ ground state, and Eu 5d-derived CB in EuS. Right panel: Predicted variation in energy over the Ln series (La, Ce, Pr, ..., Lu) of the VB maximum (□), $4f^n$ ground state (△), and 5d CB (○) for the Ln monosulfides. Filled symbols refer to occupied states. Colored areas represent Ln sulfides with metallic properties with a $4f^{n-1}5d^1$ electron configuration. Gray areas indicate semiconducting Ln sulfides for which it is energetically more favorable to localize one electron per Ln ion in the 4f shell resulting in a $4f^n5d^0$ configuration.

the Ln ion. The model predicts that the 5d states of the other Ln ions have the same energy relative to the VB and that the lowest energy 4f states are predicted by the double-seated shape, as shown.

The wide variety of electrical and optical behavior of stoichiometric Ln materials such as the LnS's is to a large extent controlled by the relative energy of the 4f and 5d states. Generally, with 5d states well above the 4f ground state, Ln materials are insulators. When 5d states are close to, but still above, the 4f ground state, semiconducting behavior dominates. When the lowest energy 5d state becomes resonant with the 4f ground state, Ln materials become critically sensitive to internal or external perturbations such as pressure that can trigger a ground-state configuration change from $4f^n5d^0$ to $4f^{n-1}5d^1$ resulting in a semiconductor to metal phase transition and a mixed Ln ion valence state. Finally, when the 5d CB has dropped below the 4f state it is energetically more favorable to delocalize one 4f electron per Ln ion in the 5d CB resulting in metallic properties.

Figure 2 shows that the model applied to LnS correctly predicts the $4f^{n-1}5d^1$ to $4f^n5d^0$ ground-state configuration crossover and the corresponding valence change from 3+ to 2+ and metal to semiconductor transition. In the first half of the Ln series it is predicted between Pm and Sm, and for the second half it is predicted between Tm and Yb. Only EuS and YbS are semiconductors with a small gap between the 4f and 5d states (gray areas in Figure 2). The other Ln sulfides (colored areas) have a metallic phase with predominantly trivalent Ln ions and itinerant electrons. The model is sufficiently accurate to predict critical behavior for SmS and TmS with almost resonant 4f and 5d states. Indeed SmS

(29) Wachter, P. *Crit. Rev. Solid State Sci.* **1972**, *3*, 189.

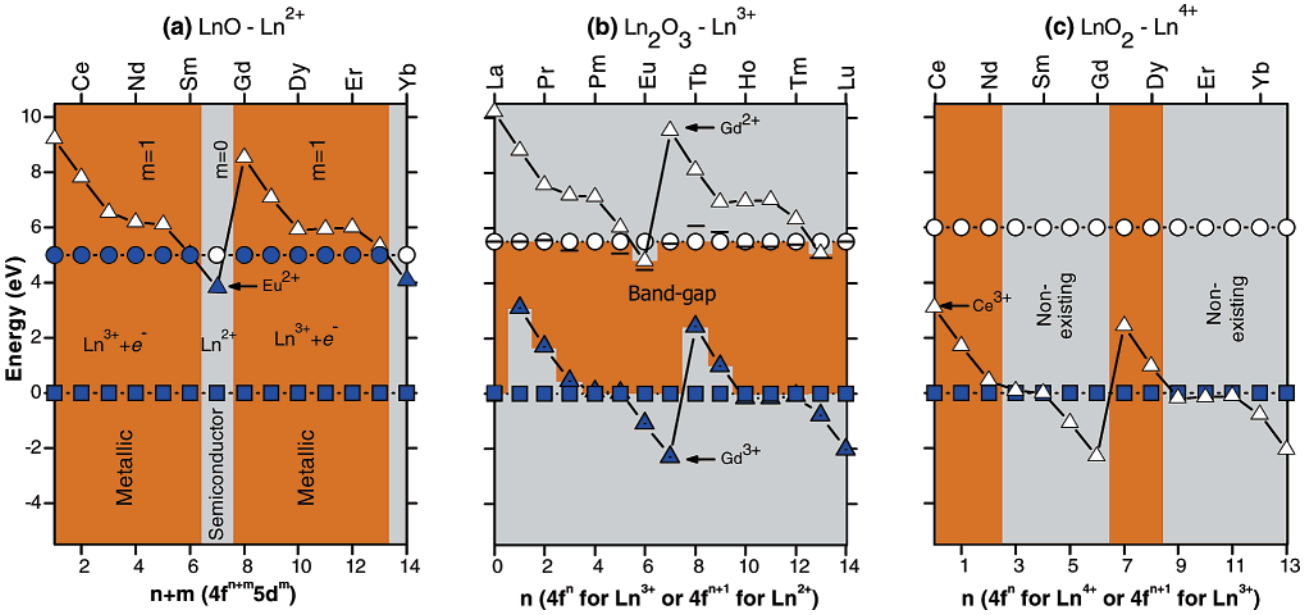

Figure 3. Predicted variation over the Ln series (La, Ce, Pr, ..., Lu) of the electronic structure of the binary Ln oxides. The VB maximum (□), the lowest energy $4f^n$ ground state (△), and the 5d CB (○) are indicated by filled or open symbols representing occupied or unoccupied states, respectively. On the basis of minimal experimental data our model correctly predicts (panel a) semiconducting or metallic behavior as well as valences and valence changes of Ln ions for the LnO's, (panel b) the nature and magnitude of band gap energies for the Ln_2O_3's, and (panel c) the chemical stability of the LnO_2's.

has earned notoriety as a result of its unique iso-structural first order semiconductor to metal phase transition at only a modest pressure of 6.5 kbar.[30] TmS has metallic properties with integer (3+) valence at low temperature but becomes mixed valence at ambient conditions.[31] Clearly the systematic behavior of the 4f and 5d states relative to the VB in Ln-doped materials can be applied to fully concentrated, stoichiometric materials as well.

3.2. Binary Lanthanide Oxides LnO, Ln_2O_3, and LnO_2. The full potential of the model for Ln materials is demonstrated by applying it to the Ln oxides LnO, Ln_2O_3, and LnO_2. These oxides have been model substances in "ab initio" theoretical calculations[14] and were chosen for their wide variety of electrical, optical, and chemical properties that cannot be explained easily. In Figure 3a the model organizes the electronic structures of the Ln mono-oxides (LnO), a system of which EuO has received by far the most attention because of a pronounced semiconductor to metal phase transition below the magnetic ordering temperature.[12] Using experimental data available[12,29] for EuO, the lowest energy 4f state is placed 1.2 eV below the 5d derived CB bottom while the VB maximum is placed 3.8 eV below the 4f state.[32] This is sufficient information to position 4f and 5d states for all the other LnO's.

Much in analogy to the LnS system (Figure 2) the model predicts semiconducting or metallic behavior (grey and colored areas, respectively) as well as valences and valence changes of the Ln ions. For most Ln oxides one electron per Ln ion is delocalized over the 5d CB states and metallic behavior is observed. For EuO and YbO, electrons no longer occupy the 5d CB but are localized in the 4f state resulting in a small band gap close to 1 eV. The model correctly predicts the ground-state configuration, including that of SmO whose electronic properties critically depend on the relative positioning of the 4f and the 5d energies. Indeed SmO is metallic.[33] No information on TmO was found, but according to Figure 3a it should be metallic like SmO.

Note that we have positioned the 4f state of Eu^{2+} 3.8 eV above the VB. In principle the VB → 4f energy in EuO can be derived from the CT energy of Eu^{3+} impurities in $Eu^{2+}O$. Unfortunately such experimental data are not available, but a reasonable estimate can be obtained from the known CT energy of Eu^{3+} impurities in SrO. Because SrO has the same structure and lattice parameters as EuO, the same position of the 4f state relative to the 2p VB is expected. Adopting the value of 3.8 eV,[32] we arrive at VB positions shown in Figure 3a. Wachter[29] has reported a much smaller VB → 4f distance of 1.1 eV; however, this disagrees with current models on CT to Eu^{3+} in oxide compounds. Although the values from Wachter were used by others[12] we believe that it is based on a misinterpretation of reflectivity data. Note that the VB energy in the LnO's do not play an important role in determining material property changes over the Ln series.

Figure 3b represents the electronic structure of the sesquioxides Ln_2O_3 (hexagonal structure type) as derived by our model. The relative position of the curves representing the VB, 4f, and 5d CB energies in Figure 3b is set by the well-established band gaps of La_2O_3 (5.4 eV) and Ce_2O_3 (2.4 eV) that are defined by a VB → 5d(CB) and a 4f → 5d(CB) transition, respectively[34] (see Figure 3b). On the basis of these two available experimental values, the lowest energy 4f and 5d states of all the other Ln ions are established. Our model correctly predicts, well within the experimental error of 0.5

(30) Jayaraman, A.; Narayanamurti, V.; Bucher, E.; Maines, R. G. *Phys. Rev. Lett.* **1970**, *25*, 1430.
(31) Wachter, P.; Kamba, S.; Grioni, M. *Physica B* **1998**, *252*, 178.
(32) Yamashita, M. *J. Lumin.* **1994**, *59*, 195.
(33) Leger, J. M.; Aimonino, P.; Loriers, J.; Dordor, P.; Coqblin, B. *Phys. Lett.* **1980**, *80*, 325.
(34) Prokofiev, A. V.; Shelykh, A. L.; Melekh, B. T. *J. Alloys Compd.* **1996**, *242*, 41.

eV, the nature and the magnitude of the band gap over the Ln series that is indicated by the colored area in Figure 3b. For La, Pm, Sm, Gd, Ho, Er, Tm, and Lu, the nature and magnitude of the band gap is the same as for La_2O_3. Smaller band gaps than La_2O_3 are predicted and found for the Ln ions with occupied 4f levels above the VB (Ce, Pr, Nd, Tb, and Dy). In those cases band gaps are determined by a 4f → 5d(CB) transition as was the case for Ce_2O_3. From Figure 3b it can be seen that the experimentally determined band gap energies,[34] indicated by the horizontal bars, for Eu_2O_3 and Yb_2O_3 are smaller than expected on the basis of a 4f → 5d(CB) transition. However, besides VB → 5d(CB) and a 4f → 5d(CB) transition, a CT transition from the VB to a 4f state of a divalent Ln ion needs to be considered. Because such a transition ends in the 4f ground state of the Ln^{2+} ion ($Ln^{3+} + e \rightarrow Ln^{2+}$), the double-seated curve of the (unoccupied) 4f states of Ln^{2+} ions in Ln_2O_3 is included in Figure 3b (open Δ symbols). This curve could have been positioned relative to the VB by using the known experimental band gap energy of Eu_2O_3. To strengthen our point that experimental data on Ln-doped materials can be used to derive properties of fully concentrated Ln materials we have placed the double-seated curve by using the CT energy[35] of Eu^{3+} as a dopant in Gd_2O_3 that has almost identical crystallographic parameters as Eu_2O_3. In this way, the experimental band gaps of Eu_2O_3 and Yb_2O_3 are well-reproduced.

Finally the Ln dioxides (LnO_2) are considered in Figure 3c. No information is available on the energy of the 4f and 5d states of Ln^{4+} ions relative to the VB in these dioxides. A well-established experimental fact is a 3 eV, CT energy from the VB to Ce^{4+} in CeO_2.[36] This VB → 4f(Ln^{4+}) transition energy can be used to position the double-seated curve representing the (unoccupied) 4f-energies of the Ln^{3+} ions in LnO_2 relative to the VB. These energies are represented by the open Δ symbols in Figure 3c. It shows that the unoccupied 4f states of Ln^{3+} ions drops into the VB twice, once in the first half of the Ln series and once in the second half. Because unoccupied levels below the top of the VB cannot exist, the trivalent Ln state is preferred and the LnO_2 phase (with Ln^{4+} ions) does not exist. According to our model this is the case for Pm to Gd and from Ho to Lu as indicated by the shaded areas in Figure 3c. Figure 3c predicts that only CeO_2, PrO_2, NdO_2, TbO_2, and DyO_2 can in principle be stable. In practice, however, only CeO_2, PrO_2, and TbO_2 have been synthesized successfully among the Ln dioxides.[37] For NdO_2 and DyO_2 the 4f states are apparently too close to the top of the VB and the Ln_2O_3 phase with trivalent Ln valence formed during synthesis.

It is interesting to observe the close similarity between the electronic structure of the three oxide systems (compare Figure 3a−c). For each oxide (LnO, Ln_2O_3, and LnO_2) the relative energies of the (occupied or unoccupied) 4f and 5d states of di- and trivalent Ln ions, represented by the circles and triangles, are approximately identical. Only a small increase (<0.5 eV) can be observed when going from LnO to Ln_2O_3 to LnO_2. The difference in electronic structure is in the filling of 4f and 5d states which obviously is different in the three oxides. This opens up the possibility to estimate, for example, the chemical stability of the LnO_2 (Figure 3c) from the metallic or semiconducting behavior of the LnO's (Figure 3a). It remains to be investigated to what extent the similarity in electronic structure as observed for the LnO, Ln_2O_3, and LnO_2 system is also observed in other Ln chalcogenide, pnictide, and halide systems other than binary.

4. Conclusion

We have presented experimental data on Ln-doped materials showing that the variation in energy of the 4f and 5d states of Ln ions relative to the VB over the Ln series (La, Ce, Pr, ..., Lu) is independent of the type of Ln material and Ln valence state. The variation in Ln 4f binding energy over the Ln series always shows the same characteristic double-seated shape. On the other hand the 5d binding energies are to a good approximation constant over the Ln series. This systematic behavior for Ln-ion-doped materials forms the basis of an empirical model for stoichiometric Ln materials such as SmS, CeO_2, or EuO. The validity of this model was successfully demonstrated by application to the well-studied Ln materials LnS, LnO, Ln_2O_3, and LnO_2, for which it correctly predicts basic material properties such as semiconducting or metallic behavior, nature, and magnitude of band gap energies and chemical stability. Once the VB and 4f and 5d CB energies of one Ln material has been established, either from theory or experiment, the model can be used to predict electronic structure of all the other corresponding Ln materials.

Because the model is relatively simple in the sense that it only needs two input parameters (representing the energy of the 4f and 5d states relative to the VB) that can be acquired from simple optical measurements, it may be frequently used in the future for other Ln materials for which little experimental data are available.

Acknowledgment. This work was supported by the Dutch Technology Foundation (STW).

CM060775S

(35) Blasse, G. *J. Electrochem.: Solid State Sci*. **1967**, *114*, 875.
(36) Marabelli, F.; Wachter, P. *Phys. Rev. B* **1987**, *36*, 1238.
(37) Adachi, G. Y.; Imanaka, N. *Chem. Rev.* **1998**, *98*, 1479.